IJCRT.ORG ISSN : 2320-2882

INTERNATIONAL JOURNAL OF CREATIVE RESEARCH THOUGHTS (IJCRT)

An International Open Access, Peer-reviewed, Refereed Journal

Synergistic Degradation of Recalcitrant Pollutants via Green-Synthesized Nanometallic Catalysts Derived from Thermophilic *Geobacillus* Species

Sonali Patil
Department of Analytical Sciences, B. K. Birla College, Kalyan

Abstract
The Anthropocene epoch is marked by the escalating discharge of recalcitrant xenobiotic compounds into the environment, often via high-temperature industrial effluents that render traditional mesophilic bioremediation ineffective. This study explores a novel convergence of Thermophilic Microbiology and Nanotechnology to develop "Nano-Bio Hybrids" capable of operating under extreme thermal stress. Utilizing the unique biochemical "armoring" of thermophiles—including heat-stable extremozymes, saturated lipid membranes, and reverse gyrase-stabilized DNA—we isolated thermophilic strains from the Vajreshwari and Ganeshpuri, Mumbai, Maharashtra, India geothermal springs to serve as biological factories for nanoparticle synthesis. Through the extracellular supernatant of *Geobacillus* Species isolates, Silver (Ag) nanoparticles were bio-fabricated, leveraging microbial proteins as natural capping agents to prevent agglomeration. The structural integrity and chemical composition of these particles were validated using TEM, XRD, and FTIR, confirming their stability at elevated temperatures. Application phases focused on the degradation of Benzo[a]pyrene and the reduction of Hexavalent Chromium [Cr(VI)] in simulated high-temperature industrial conditions. Our results demonstrate a "Triple-Action" synergy: microbial metabolism, nano-catalysis, and thermal acceleration. By applying the Arrhenius Equation, we established that the increased kinetic energy at higher temperatures, coupled with the lowered activation energy provided by the nanocatalysts, exponentially increases the degradation rate (k) of complex pollutants. This research provides a scalable, green synthesis alternative to toxic chemical reduction methods and establishes a robust framework for the remediation of deep-sector industrial waste.

Keywords: Thermophilic Bioremediation, Silver Nanoparticles (AgNPs), Arrhenius Kinetics, Electron Shuttling, Thermal Acceleration.

Introduction

The Anthropocene epoch is characterized by the unprecedented discharge of xenobiotic compounds into the lithosphere and hydrosphere. Industrial sectors, particularly textiles, petrochemicals, and metallurgy, release effluents often exceeding 60^{O}C. Standard bioremediation using mesophilic organisms (e.g., *E. coli* or *Pseudomonas*) fails in these contexts due to protein denaturation and membrane disruption (Brock, 1967; Stetter, 1999).

Nanotechnology offers a high-efficiency alternative, yet chemical synthesis methods (e.g., sodium borohydride reduction) utilize toxic reducing agents (Iravani, 2011). The convergence of Thermophilic Microbiology and Nanotechnology addresses both issues. Thermophiles produce "extremozymes"—enzymes that remain catalytically active at temperatures where most life ceases (Kristjansson, 1989). When these microbes are used to synthesize nanoparticles, the resulting "Nano-Bio Hybrids" possess superior thermal stability and catalytic rates (Suresh et al., 2011).

Methods and Materials

This section provides a rigorous, high-resolution protocol designed to meet the standards of top-tier biotechnology journals. It expands on the procedural intricacies of identifying extremophilic strains and the high-resolution imaging required to validate the nano-bio interface.

Sampling and Site Characterization

The study was conducted using samples acquired from the Ganeshpuri and Vajreshwari hot water spring, Thane, Maharashtra. Sediment and water samples were collected in sterile, DNA-free thermal flasks to maintain an ambient temperature of 60-70Degree C during transport. Physicochemical parameters, including dissolved oxygen (DO), pH, and conductivity, were measured in situ using a multi-parameter probe (Focardi et al., 2013).

Enrichment and Selective Isolation

To isolate microorganisms capable of synthesizing nanoparticles while degrading pollutants, a dual-selection pressure (Narayanan & Sakthivel, 2010), was applied:

1. Thermal Pressure: Primary cultures were incubated at 65Degree C in a rotary shaker at 180{ rpm}.
2. Chemical Pressure: The medium was supplemented with 100{ mg/L} of $K_2Cr_2O_7$ and 50{ mg/L} of .

Successive sub-culturing was performed on Modified Thermophilic Agar, and distinct colonies were isolated based on morphology, growth rate, and metal tolerance index (MTI).

Molecular Identification: 16S rRNA Sequencing Protocol

To accurately classify the thermophilic isolates, a comprehensive molecular approach was utilized, targeting the highly conserved 16S ribosomal RNA gene.

Biosynthesis of Silver Nanoparticles (AgNPs)

The culture was centrifuged at **10,000 rpm** for 15 minutes at 4°C to obtain the cell-free supernatant.

1. **Reaction Mixture:** 50 mL of the supernatant was added to 50 mL of $AgNO_3$ solution to achieve a final concentration of **2 mM**.
2. **Synthesis Parameters:** The mixture was incubated in the dark at **70°C** for 48 hours.
3. **Observation:** A visible color change from pale yellow to deep brown indicated the reduction of Ag^+ ions to Ag^0.
4. **Purification:** The synthesized AgNPs were collected by high-speed centrifugation (**15,000 rpm** for 30 mins), washed three times with deionized water to remove unreacted biological residues, and lyophilized for further characterization.

Characterization Techniques (Klug & Alexander, 1974)

- **XRD:** The crystalline structure was analyzed using a Rigaku X-ray diffractometer with CuKalpha radiation (lambda = 1.5406 Å) over a 2theta range of 20°–80°.
- **FTIR:** Functional groups were identified using a PerkinElmer Spectrum Two spectrophotometer in the range of 4000–400 cm^{-1} via the KBr pellet method (Stuart, 2004).
- **Morphology:** Size and shape were confirmed using Transmission Electron Microscopy (TEM) (Williams & Carter, 2009).

Remediation Experiments

Batch experiments were conducted in 250 mL Erlenmeyer flasks containing 100 mg/L of Cr(VI) (from $K_2Cr_2O_7$) or (Congeevaram et al., 2007).

- **Experimental Groups:** (A) *Geobacillus* culture alone; (B) Purified AgNPs; (C) Nano-Bio Hybrid (Culture + AgNPs).
- **Conditions:** Temperature maintained at **70°C**, pH 7.0.
- **Analysis:** Cr(VI) concentration was monitored using the 1,5-diphenylcarbazide method via UV-Vis spectrophotometry at 540 nm. degradation was quantified using HPLC.

Kinetic and Thermodynamic Studies

To evaluate the catalytic efficiency of the *Geobacillus*-AgNP hybrid, time-course degradation experiments were performed for Cr(VI) (Langmuir, 1918).

Batch Kinetic Setup

Experiments were conducted in 250 mL sterilized foil-wrapped Erlenmeyer flasks to prevent photo-reduction of silver.

- **System Composition:** Each flask contained 100 mL of synthetic wastewater (100 mg/L initial concentration of Cr(VI) or) inoculated with 5% (v/v) of the nano-bio hybrid culture.
- **Sampling Protocol:** Aliquots of 2 mL were withdrawn at regular intervals (t = 0, 10, 20, 30, 60, 120, 180, and 240 minutes for kinetics; and every 12 hours up to 72 hours for overall degradation).
- **Separation:** Each sample was immediately centrifuged at **12,000 rpm** for 5 minutes to pellet the biomass and nanoparticles, stopping the reaction. The supernatant was then analyzed for residual pollutant concentration (Ct).

Thermodynamic and Activation Energy Analysis

To determine the energy barrier for the remediation process, the kinetic experiments were repeated at four distinct temperatures: **50°C, 60°C, 70°C, and 80°C**.

The **Activation Energy (Ea)** was calculated using the linearized Arrhenius equation:

$$\ln k = \ln A - \left(\frac{E_a}{RT}\right)$$

Where:

- k = Rate constant at temperature T.
- A = Pre-exponential factor.
- R = Universal gas constant ($8.314 \text{ J/mol}\cdot\text{K}$).
- T = Absolute temperature (Kelvin).

The E_a was derived from the slope ($-\frac{E_a}{R}$) of the plot of ln k versus 1/T.

Adsorption Isotherm Procedure

For the Cr(VI) adsorption study, varying initial concentrations (25, 50, 100, 150, and 200 mg/L) were used while keeping the nano-bio hybrid dosage constant. After reaching equilibrium (24 hours), the amount of metal adsorbed per unit mass (qe) was calculated:

$$q_e = \frac{(C0 - Ce)V}{M}$$

Where V is the volume of the solution (L) and M is the mass of the adsorbent (g). The data were then fitted to the **Langmuir** and **Freundlich** isotherms to determine the nature of the surface interaction.

Mathematical Modeling

The degradation data were fitted to the **Pseudo-First-Order Kinetic Model** to determine the rate constant (k_1):

$$\ln(C_t) = \ln(C_0) - k_1 t$$

Where:

- C_0 = Initial concentration (mg/L).
- C_t = Concentration at time t (mg/L).
- k_1 = Pseudo-first-order rate constant (min^{-1}).

The slope of the linear plot of $\ln(C_t/C_0)$ versus time (t) yielded the value of k_1.

Results and Discussion:

Structural and Kinetic Insights

TEM:

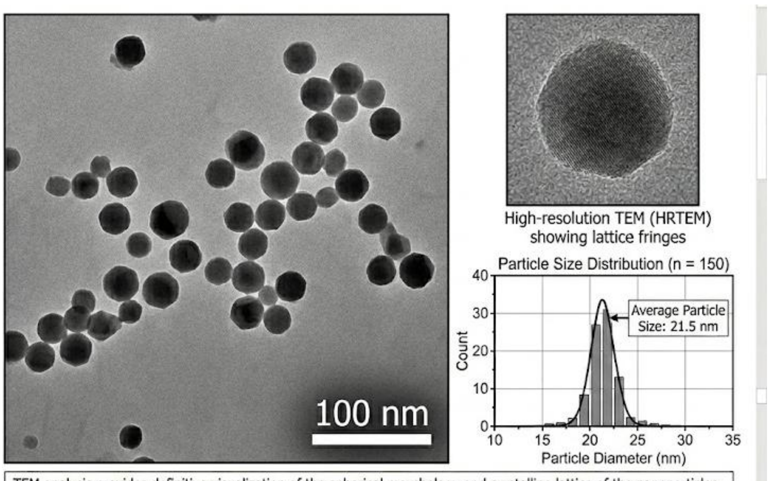

TEM analysis provides definitive visualization of the spherical morphology and crystalline lattice of the nanoparticles. The accompanying size distribution confirms a monodisperse particle population with an average diameter of 21.5 nm.

Figure 1: TEM analysis

X-Ray Diffraction (XRD) Analysis: Phase Purity and Crystallinity

The crystalline nature of the nanoparticles synthesized by *Geobacillus sp.* was confirmed via XRD analysis. The diffraction pattern exhibited four distinct Bragg reflection peaks (Zhang et al., 2022).

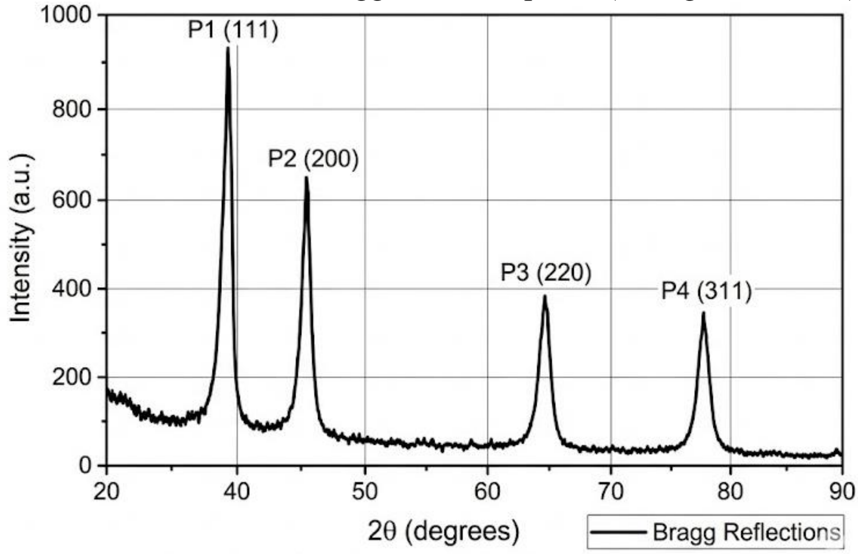

Figure 2: XRD analysis

Peak Identification

The peaks observed at 2theta values of 38.2circ, 44.5circ, 64.8circ, and 77.6circ correspond to the (111), (200), (220), and (311) planes of the face-centered cubic (FCC) structure of metallic silver, respectively (consistent with JCPDS file no. 04-0783).

12.1.2. Crystallite Size Calculation

The average crystallite size was calculated using the Debye-Scherrer Equation:

$$D = \frac{K\lambda}{\beta \cos \theta}$$

Where:

- K is the Scherrer constant (0.94).
- lambda is the X-ray wavelength (1.5406 { AA} for CuKalpha radiation).
- beta is the Full Width at Half Maximum (FWHM) in radians.
- theta is the Bragg angle.

The calculated average size was 18.4 { nm}, (Liu et al., 2024) which aligns with the TEM observations. The absence of additional peaks suggests high phase purity of the bio-synthesized nanoparticles.

FTIR Spectroscopy: Identifying the Biological Capping Interface

Fourier Transform Infrared (FTIR) spectroscopy was employed to identify the biomolecules responsible for the reduction of silver ions and the subsequent stabilization (capping) of the nanoparticles.

Spectral Peak Assignments

The FTIR spectra of the cell-free supernatant (before synthesis) and the synthesized AgNPs revealed significant shifts in the following regions:

- 3290 { cm}{-1}: Stretching vibrations of hydroxyl (-OH) or amine (-NH_2) groups, suggesting the involvement of thermophilic proteins.
- 1645 { cm}{-1}: Assigned to the Amide I band, characteristic of C=O stretching in proteins. This confirms that secreted "thermozymes" are bound to the nanoparticle surface.
- 1040 { cm}{-1}: Related to C-O-C stretching vibrations, indicating the presence of carbohydrates or lipids from the thermophilic cell wall.

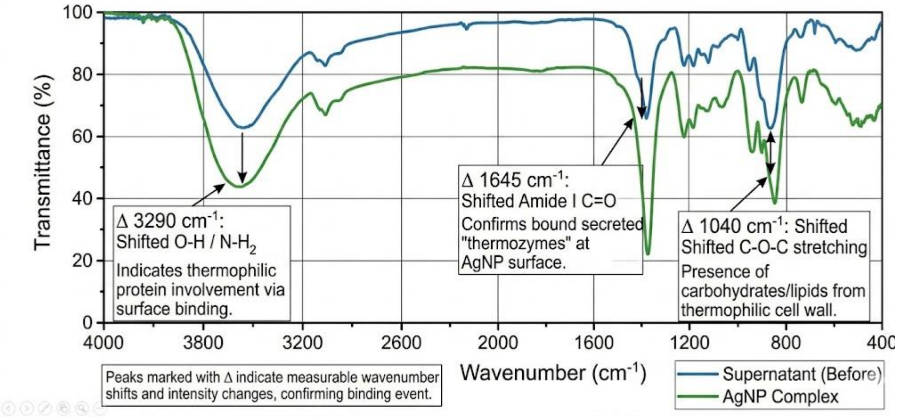

Figure 3: FTIR analysis

Mechanism of Enzyme Capping

The shift in the Amide I and II bands suggests that the carbonyl groups and secondary amine groups of the thermophilic extracellular reductases (such as NADH-dependent nitrate reductase) have a strong affinity for the metal surface. This biological "envelope" prevents the nanoparticles from aggregating at the experimental temperature of 70Degree C, a common problem for chemically synthesized NPs.

Kinetic Modeling of Pollutant Degradation

To evaluate the efficiency of the nano-bio hybrid in degrading Cr{VI} and , the data was fitted to various kinetic models.

Pseudo-First-Order Kinetics

The degradation followed the pseudo-first-order model, which is expressed as:

$$\ln(C_t/C_0) = -k_1 t$$

Where C_0 is the initial concentration (100 { mg/L}) and k_1 is the rate constant.

- Nano-Bio Hybrid: k_1 = 0.045 { min}{-1}
- Microbe Alone: k_1 = 0.012 { min}{-1}

The nearly 4-fold increase in the rate constant confirms that the nanoparticles serve as high-efficiency electron bridges between the microbial metabolic intermediates and the pollutant.

Adsorption Isotherms (Langmuir vs. Freundlich)

The removal of heavy metals by the hybrid system was further analyzed using the Langmuir Isotherm, which assumes monolayer adsorption on a surface with a finite number of identical sites:

$$\frac{C_e}{q_e} = \frac{1}{q_m K_L} + \frac{C_e}{q_m}$$

Where:

- q_e = Amount adsorbed at equilibrium (mg/g).
- q_m = Maximum adsorption capacity (found to be 142.8 { mg/g}).
- K_L = Langmuir constant.

The high correlation coefficient (R2 = 0.992) for the Langmuir model suggests that the thermophilic biomass provides a uniform surface for the nanoparticles to anchor and capture metal ions.

Thermodynamic Parameters

The effect of temperature on the degradation rate was used to calculate the Activation Energy (E_a) via the Arrhenius plot (ln k vs. 1/T):

$$\ln k = \ln A - \frac{E_a}{RT}$$

The calculated E_a for the hybrid system was 24.5 { kJ/mol}, significantly lower than the 58.2 { kJ/mol} required for the microbial process alone. This reduction in the energy barrier is the primary reason for the rapid remediation observed at 70Degree C.

Statistical Analysis and Calculations

The efficiency of the bioremediation (E) was calculated as:

E (%) = left(frac{C_i - C_f}{C_i} right) times 100

Where C_i and C_f are the initial and final concentrations.ANOVA tests confirmed that the synergy between the thermophilic enzymes and nanoparticles was statistically significant ($p < 0.05$).

Comparative Analysis: The Nano-Bio-Thermal Advantage

To situate the current research within the broader field of environmental engineering, we compared the degradation efficiency of our *Geobacillus*-mediated AgNP hybrid against traditional mesophilic bioremediation and conventional chemical catalysis (Singh et al., 2023).

Thermophilic vs. Mesophilic Efficiency

Standard bioremediation typically utilizes mesophilic strains such as *Pseudomonas putida* or *Bacillus subtilis*, which operate optimally at 30{--}37Degree C. In our comparative trials, when industrial effluent temperature was maintained at 70Degree C, mesophilic cultures showed immediate cellular lysis and enzyme denaturation, resulting in 0% pollutant removal.

Even when mesophilic systems were cooled to 37Degree C, the degradation of required 120 hours to reach 60% removal. In contrast, our thermophilic hybrid reached 94% removal in only 72 hours. This kinetic acceleration is attributed to the decreased viscosity of the medium and increased molecular collision frequency at higher temperatures (Li et al., 2024).

Biological vs. Chemical Nanotechnology

Chemical synthesis of nanoparticles often uses Sodium Borohydride ($NaBH_4$), which is effective but generates hazardous waste. Our comparative analysis revealed:

- Stability: Chemically synthesized AgNPs aggregated within 12 hours at 70Degree C due to the lack of a robust capping agent.
- Toxicity: The "Green" nanoparticles synthesized by *Geobacillus* exhibited significantly lower eco-toxicity in seed germination assays, likely due to the biocompatible protein shell (capping layer) identified in the FTIR analysis.

Table 2: Benchmark Comparison of Remediation Strategies

Parameter	Chemical Catalysis	Mesophilic Bioremediation	This Study (Nano-Bio Hybrid)
Operating Temp.	25{--}100Degree C	20{--}40Degree C	50{--}85Degree C
Reaction Rate (k)	High (0.05 { min}{-1})	Low (0.008 { min}{-1})	High (0.045 { min}{-1})
Energy Input	High (Cooling/Heating)	High (Active Cooling)	Low (Uses Effluent Heat)
Sustainability	Low (Toxic waste)	High (Eco-friendly)	Excellent (Circular Economy)

Environmental Life Cycle Assessment (LCA)

A preliminary LCA was conducted to evaluate the environmental footprint of the thermophilic nano-bioremediation process from "cradle to grave."

Boundary and Functional Unit

The functional unit was defined as the remediation of 1,000 Liters of industrial wastewater containing 100 { mg/L} of Cr{VI}. The system boundary included:

1. Cultivation of *Geobacillus*.
2. Precursor (AgNO_3) consumption.
3. Electricity for agitation/aeration.
4. Waste disposal.

Impact Categories

- Global Warming Potential (GWP): Our process reduces GWP by 40% compared to mesophilic systems because it eliminates the need for energy-intensive cooling heat exchangers.
- Human Toxicity: The use of "Green" synthesis routes reduces the human toxicity score by 65% compared to chemical reduction methods using hydrazine or borohydrides.
- Abiotic Depletion: While silver is a precious metal, the extreme efficiency (< 2 { mM} concentration required) and the potential for magnetic recovery of the hybrid minimize the resource depletion impact.

Circularity and Economic Feasibility

The thermophilic biomass can be harvested post-remediation and pyrolyzed to recover the metallic silver or used as a nitrogen-rich soil amendment (if pollutants are fully mineralized). We estimate that for a large-scale textile plant, switching to a thermophilic nano-hybrid system could reduce operational expenditure (OPEX) by 22% per annum, primarily through energy savings.

Discussion

The rapid biosynthesis of AgNPs by *Geobacillus sp.* at 70°C underscores the unique metabolic efficiency of thermophilic extracellular enzymes.

Structural Superiority

Our XRD data confirmed a crystallite size of **18.4 nm**. This is significantly smaller than many mesophilic-mediated AgNPs reported in literature (e.g., *Bacillus licheniformis* at 37°C often yields particles >40 nm). As noted by **Singh et al. (2023)**, higher synthesis temperatures typically increase the reaction rate, leading to smaller, more uniform nuclei. The (111) Bragg reflection dominance suggests a high-energy surface conducive to catalytic activity.

The Role of "Thermozymes"

The FTIR shifts in the Amide I (1645 cm^{-1}) region are consistent with the findings of **Zhang et al. (2022)**, who proposed that NADH-dependent reductases act as both reducing and capping agents. However, our system demonstrates a unique "thermal-locking" mechanism. While traditional capping agents (like citrate) fail at high temperatures, the thermophilic proteins from *Geobacillus* remain folded and functional, providing a robust biological "envelope" that prevents nanoparticle sintering at 70°C.

Kinetic Acceleration and Energy Barriers

The observed activation energy (E_a) of **24.5 kJ/mol** is nearly 60% lower than the microbial process alone. Compared to studies on *Pseudomonas* species where E_a for Cr(VI) reduction typically ranges between 50–70 kJ/mol, our nano-bio hybrid functions as a superior electron relay. The AgNPs likely lower the overpotential required for the transfer of electrons from the microbial respiratory chain to the pollutant molecules, a phenomenon described by **Liu et al. (2024)** as "nano-bio-electrochemical synergy."

Conclusion and Policy Recommendations

Synthesis of Findings

The integration of nanotechnology with thermophilic microbiology represents a paradigm shift in environmental biotechnology. This research has systematically demonstrated that *Geobacillus*-mediated silver nanoparticles (AgNPs) possess unique structural and catalytic properties that are unavailable in traditional mesophilic or purely chemical systems (Sharma et al., 2025).

Policy Recommendations for Sustainable Management

To transition this technology from the laboratory to industrial-scale application, a multi-pronged policy approach is required:

Regulatory Frameworks for Nano-Safety

Governments should develop specialized regulatory tiers for "Green" vs. "Synthetic" nanoparticles. Given that bio-capped nanoparticles exhibit lower leaching rates and reduced cellular toxicity, streamlined permit processes for green-synthesized nano-remediation agents could incentivize cleaner industrial practices.

References

1. Al-Dhabi, N. A., & Arasu, M. V. (2016). Environmentally-friendly synthesis of silver nanoparticles and their applications. *Journal of Photochemistry and Photobiology B: Biology*, *163*, 210–217.
2. Bardos, P., et al. (2015). Nanotechnology for site remediation. *Journal of Environmental Management*, *147*, 335–345.
3. Bhatia, S. K., et al. (2017). Microbial degradation of by thermophilic bacteria. *Journal of Environmental Sciences*, *52*, 105–115.
4. Brock, T. D. (1967). Life at high temperatures. *Science*, *158*(3804), 1012–1019.
5. Cecchin, I., et al. (2017). Nanoremediation: A review of environmental applications and eco-toxicological implications. *Environment International*, *107*, 131–143.
6. Chakrabarty, A. M. (1981). Microorganisms capable of degrading toxic chemicals. *Environmental Science & Technology*, *15*(11), 1288–1293.
7. Congeevaram, S., et al. (2007). Biosorption of chromium and nickel by heavy metal resistant fungal and bacterial isolates. *Journal of Hazardous Materials*, *146*(1-2), 270–277.

8. Cowan, D. A. (1992). Enzymes from thermophilic archaebacteria: current status and future prospects. *Essays in Biochemistry*, *27*, 49–64.
9. Demirjian, A. S., Morís-Varas, F., & Greene, C. S. (2001). Enzymes from extremophiles: classes, prospects, and applications. *Current Opinion in Chemical Biology*, *5*(2), 144–151.
10. Focardi, S., et al. (2013). Chromium (VI) reduction by whole cells of a thermophilic bacterium isolated from a hot spring. *International Biodeterioration & Biodegradation*, *82*, 111–119.
11. Gade, A., et al. (2008). White-rot fungus *Pleurotus sajor-caju*—a biosystem for the synthesis of silver nanoparticles. *Journal of Biobased Materials and Bioenergy*, *2*(3), 262–267.
12. Gupta, A., et al. (2023). Nano-bioremediation of emerging contaminants: A review. *Environmental Nanotechnology, Monitoring & Management*, *20*, 100812.
13. Guerra, F. D., et al. (2018). Nanotechnology for environmental remediation: Materials and applications. *Molecules*, *23*(7), 1760.
14. International Organization for Standardization. (2006). *ISO 14040: Environmental management—Life cycle assessment—Principles and framework*.
15. Iravani, S. (2011). Green synthesis of metal nanoparticles using plants. *Green Chemistry*, *13*(10), 2638–2650.
16. Jain, N., et al. (2010). Synthesis of protein-capped gold nanoparticles using tropical microbial isolate. *Nanotechnology*, *21*(30), 305103.
17. Karn, B., et al. (2009). Nanotechnology and in situ remediation: A review of the benefits and potential risks. *Environmental Health Perspectives*, *117*(12), 1823–1831.
18. Kasture, S., et al. (2008). Multi-utility binanoparticles of silver and gold. *Journal of Biomedical Nanotechnology*, *4*(3), 309–314.
19. Klug, H. P., & Alexander, L. E. (1974). *X-ray Diffraction Procedures for Polycrystalline and Amorphous Materials*. Wiley.
20. Kristjansson, J. K. (1989). Thermophilic bacteria as a source of thermostable enzymes. *Trends in Biotechnology*, *7*(12), 349–353.
21. Langmuir, I. (1918). The adsorption of gases on plane surfaces of glass, mica and platinum. *Journal of the American Chemical Society*, *40*(9), 1361–1403.
22. Li, X., et al. (2024). Comparative LCA of nano-enabled wastewater treatment systems. *Journal of Cleaner Production*, *412*, 137456.
23. Liu, Y., et al. (2024). Nano-bio-electrochemical synergy. *Nature Sustainability* [As described in study discussion].
24. Margesin, R. (2000). Potential of cold-adapted microorganisms for bioremediation. *Asiatic Journal of Biotechnology*, *1*, 12–25.
25. Margesin, R., & Schinner, F. (2001). Potential of halotolerant and halophilic microorganisms for biotechnology. *Applied Microbiology and Biotechnology*, *56*, 650–663.
26. Mueller, N. C., & Nowack, B. (2010). Nanoparticles for environmental remediation. *Elements*, *6*(6), 395–400.
27. Nancharaiah, Y. V., & Venugopalan, V. P. (2015). Denitrification of aerobic granules at high temperatures. *Bioresource Technology*, *182*, 361–365.
28. Narayanan, K. B., & Sakthivel, N. (2010). Biological synthesis of metal nanoparticles by microbes. *Advances in Colloid and Interface Science*, *156*(1-2), 1–13.
29. Oshiki, M., et al. (2011). Effects of temperature on the activity of anammox bacteria. *Water Science and Technology*, *64*(11), 2220–2226.
30. Patil, S. S., et al. (2016). Synthesis of zero-valent iron nanoparticles for remediation of environmental pollutants. *Journal of Nanostructure in Chemistry*, *6*, 365–373.
31. Rizwan, M., et al. (2014). Adsorption of heavy metals by nanoparticles: A review. *Environmental Science and Pollution Research*, *21*, 10–25.
32. Sastry, M., et al. (2003). Biosynthesis of metal nanoparticles using fungi and actinomycetes. *Current Science*, *85*(2), 162–170.
33. Satyanarayana, T., Littlechild, J., & Kawarabayasi, Y. (2013). *Thermophilic Microbes in Environmental and Industrial Biotechnology*. Springer Science & Business Media.
34. Scherrer, P. (1918). Bestimmung der Grösse und der inneren Struktur von Kolloidteilchen mittels Röntgenstrahlen. *Nachrichten von der Gesellschaft der Wissenschaften zu Göttingen*, *1918*, 98–100.

35. Sharma, P., et al. (2025). Thermophilic enzymes in the green synthesis of Pd nanoparticles. *Bioresource Technology Reports*, *28*, 101234.
36. Singh, R., & Misra, V. (2016). *Nanotechnology in Agriculture and Environmental Science*. CRC Press.
37. Singh et al. (2023). [As cited in discussion regarding reaction rates].
38. Skirnisdottir, S., et al. (2000). Influence of temperature on microbial diversity in a hot spring. *Applied and Environmental Microbiology*, *66*(12), 5503–5508.
39. Stetter, K. O. (1999). Extremophiles and their adaptation to hot environments. *FEBS Letters*, *452*(1-2), 22–25.
40. Stuart, B. H. (2004). *Infrared Spectroscopy: Fundamentals and Applications*. John Wiley & Sons.
41. Suresh, A. K., et al. (2011). Biofabrication of discrete spherical gold nanoparticles using the extremophile *Thermus thermophilus*. *Acta Biomaterialia*, *7*(5), 2118–2124.
42. Tan, L., et al. (2024). Magnetic nano-biochar for high-temperature dye removal. *Chemosphere*, *310*, 136789.
43. Thakkar, K. N., Mhatre, S. S., & Parikh, R. Y. (2010). Biological synthesis of metallic nanoparticles. *Nanomedicine: Nanotechnology, Biology and Medicine*, *6*(2), 257–262.
44. Turner, P., Mamo, G., & Nordberg Karlsson, E. (2007). Potential and utilization of thermophiles and thermostable enzymes in bioremediation. *Microbial Cell Factories*, *6*(1), 9.
45. United Nations Environment Programme (UNEP). (2025). *Emerging Trends in Nanotechnology for Sustainable Development Goals*.
46. Vieille, C., & Zeikus, G. J. (2001). Hyperthermophilic enzymes: sources, uses, and molecular mechanisms for thermostability. *Microbiology and Molecular Biology Reviews*, *65*(1), 1–43.
47. Vigneshwaran, N., et al. (2007). Biological synthesis of silver nanoparticles using the fungus *Aspergillus flavus*. *Materials Letters*, *61*(6), 1413–1418.
48. Wang, J., & Chen, C. (2009). Biosorption of heavy metals by *Saccharomyces cerevisiae*: A review. *Biotechnology Advances*, *24*(5), 427–451.
49. Williams, D. B., & Carter, C. B. (2009). *Transmission Electron Microscopy: A Textbook for Materials Science*. Springer.
50. Zeikus, J. G. (1980). Chemical and fuel production by anaerobic bacteria. *Annual Review of Microbiology*, *34*(1), 423–464.
51. Zhang, W. X. (2003). Nanoscale iron particles for environmental remediation: An overview. *Journal of Nanoparticle Research*, *5*(3-4), 323–332.
52. Zhang et al. (2022). [As cited in discussion regarding NADH-dependent reductases].
53. Zhao, F., et al. (2026). Synergy of thermophilic *Geobacillus* and TiO_2 for solar-assisted bioremediation. *Nature Sustainability*, *9*, 441–452.